

Article

Looking back to lower-level information in few-shot learning

Zhongjie Yu¹ and Sebastian Raschka^{1,*†}¹ University of Wisconsin-Madison, Department of Statistics

* Correspondence: sraschka@wisc.edu

† Current address: 1300 University Ave, Medical Sciences Building, Madison, WI 53706, USA

Received: date; Accepted: date; Published: date

Abstract: Humans are capable of learning new concepts from small numbers of examples. In contrast, supervised deep learning models usually lack the ability to extract reliable predictive rules from limited data scenarios when attempting to classify new examples. This challenging scenario is commonly known as few-shot learning. Few-shot learning has garnered increased attention in recent years due to its significance for many real-world problems. Recently, new methods relying on meta-learning paradigms combined with graph-based structures, which model the relationship between examples, have shown promising results on a variety of few-shot classification tasks. However, existing work on few-shot learning is only focused on the feature embeddings produced by the last layer of the neural network. In this work, we propose the utilization of lower-level, supporting information, namely the feature embeddings of the hidden neural network layers, to improve classifier accuracy. Based on a graph-based meta-learning framework, we develop a method called Looking-Back, where such lower-level information is used to construct additional graphs for label propagation in limited data settings. Our experiments on two popular few-shot learning datasets, *miniImageNet* and *tieredImageNet*, show that our method can utilize the lower-level information in the network to improve state-of-the-art classification performance.

Keywords: Machine learning; deep learning; few-shot learning; meta-learning; graph neural networks; image classification

1. Introduction

Deep learning (DL) is already ubiquitous in our daily lives, including image-based object detection [1], face recognition [2], and medical imaging and healthcare [3]. While DL is outperforming traditional machine learning methods in these aforementioned application areas [4], a major downside of DL is that it requires large amounts of data to achieve good performance [5]. Few-shot learning (FSL) is a subfield of DL that focuses on training DL models under scarce data regimes, thereby opening possibilities for applying DL to new problem areas where the amount of labeled data is limited.

In FSL settings, datasets are comprised of large numbers of categories (i.e., class labels), but only a few images per class are available. The main objective of FSL is the design of methods that achieve good generalization performance from the limited number of images per category. The overarching concept of FSL is very general and applies to different data modalities. However, most FSL research is focused on image classification [6] so that we will use the terms *examples* and *images* (in a supervised learning context) interchangeably.

Most FSL methods use an episodic training strategy known as meta-learning [7], where a meta-learner is trained on (classification) tasks with the goal to learn to perform well on new, unseen tasks. While many of the most recent FSL methods are based on episodic meta-learning [8–11], another successful approach to FSL is the use of transfer learning, where models are trained on large datasets and then appropriately transferred to smaller datasets that contain the novel target classes [12–14].

Apart from recent developments in FSL, many researchers have recently proposed methods for implementing graph neural networks to extend deep learning approaches for graph-structured data. In this context, graphs are used as data structures for modeling the relationships (edges) between data instances (nodes) [15–19]. Since FSL methods are centered around modeling relationships between the examples in the support and query datasets, graph neural networks have also gained a growing interest in FSL research [20–22]. Graph neural networks can be computationally prohibitive on large datasets. However, we shall note that one of the significant characteristics of FSL is that datasets for meta-training and meta-testing contain only "few" examples per class, such that the computational cost of graph construction becomes small in FSL.

Previous research has shown that FSL can be improved by incorporating additional information. For instance, unlabeled data [23–25] and additional modalities (e.g., textual information describing the images to be classified) [26,27] could improve the predictive performance of FSL models. While the aforementioned works showed that additional *external* information benefits FSL, we raise the question of whether additional *internal* information can be useful as well.

While the incorporation of additional information can be beneficial, the utilization of additional *internal* information is not very common in FSL research, and only two recent research papers explored this approach [28,29]. In these works, the researchers expanded the feature embedding vectors of the data inputs (i.e., images), obtained from the last layer in the neural network, to higher-dimensional embeddings. These higher-dimensional embeddings were split into several smaller vectors, such that multiple embedding vectors correspond to the same image. In the DN4 model proposed by Li et al. [28], the last layer’s feature embeddings were expanded to form many local descriptors. The dense classification network by Lifchitz et al. [29] expanded the feature embeddings to three separate vectors that are used for computing the cross-entropy loss during training.

When it comes to utilizing additional internal information, both DN4 [28] and the dense classification network [29] only considered the last layer’s information. In contrast to existing work on FSL, we consider additional information that is hidden in the earlier layers of the neural network. We hypothesize that such internal information benefits an FSL model’s predictive performance. More specifically, the extra information hidden in the network considered in this work is comprised of the feature embeddings that can be obtained from layers before the last layer. We propose using a graph structure to integrate this lower-level information into the neural network.

We refer to the FSL method proposed in this paper as *Looking-Back*, because unlike DN4 [28] and the dense classification network [29], this method is looking back at lower-level information rather than focusing on the final layer’s feature embeddings alone. During training, the lower-level information is expected to help the meta-learner to absorb more information overall. Although this lower-level information may not be as useful as the embedding vectors obtained from the last layer, we hypothesize that the lower-level information has a positive impact on the meta-learner. To test this hypothesis, we experiment with the popular Conv-64F model [28] as a backbone, and we follow the TPN method [21] for graph construction and label propagation.

Besides the feature embeddings of the last layer, the previous layers’ feature embeddings (i.e., lower-level information) are also used for computing the pair-wise similarities between the inputs, based on relational network structures, which differs from the original TPN implementation [21]. In the Looking-Back method, three groups of pair-wise similarity measures are computed. The similarity scores between all support and query images in one episode amount to three separate graph Laplacians, which are used for iterative label propagation, to generate three separate cross-entropy losses. As the experimental results indicate, the losses from lower-level features are used during meta-training to enhance the performance of the meta-learner. After meta-training, we adopt the last layer’s feature embeddings for testing on new tasks (i.e., images with class labels that are not seen during training) in a transductive

fashion. As the experimental results reveal, the resulting FSL models have a better predictive performance on new, unseen tasks compared to models generated by meta-learners that don't utilize lower-level information.

The contributions of this work can be summarized as follows:

1. We propose an FSL meta-learner, Looking-Back, that utilizes lower-level information from hidden layers, which is different from existing FSL methods that only use feature embedding of the last layer during meta-training.
2. We implement our Looking-Back method using a graph neural network, which fully utilizes the advantage of graph structures for few-shot learning to absorb the lower-level information in the hidden layers of the neural network.
3. We evaluate our proposed Looking-Back method on two popular FSL datasets, *miniImageNet* and *tieredImageNet*, and achieve new state-of-the-art results, providing supporting evidence that using lower-level information could result in better meta-learners in FSL tasks.

2. Related Work

In this section, we discuss the recent developments in FSL with a focus on methods related to our work. We group these related FSL methods into two main categories, meta-learning-based approaches and transfer learning-based approaches.

2.1. Meta-learning

FSL, based on meta-learning, typically uses episodic training strategies. In each episode, the meta-learner is trained on a meta-task, which can be thought of as an image classification task. During training, these tasks are drawn randomly from the training dataset across the episodes. During the model evaluation, tasks are chosen from a separate test dataset, which consists of images from novel classes that are not contained in the training dataset.

In N -way- k -shot FSL, when a meta-learner is trained on several tasks sampled from the training dataset, each training task is subdivided into a support set and a query set. Each task consists of N unique class labels, and the support set consists of k labeled images per class. Utilizing the support set, the model learns to predict the image labels in the query set. After training, the meta-learner is then evaluated on new tasks sampled from the test set. Similar to the training tasks, each new task consists of N unique class labels with k images (in the support set) each. However, to assess how well the meta-learner performs on new tasks, the classes in the test dataset are not overlapping with the classes in the training set.

Based on the general FSL meta-learning framework described above, we can divide meta-learning approaches further into metric-, optimization-, and graph-based meta-learning, which we discuss in the following subsections.

2.1.1. Metric-based Meta-learning

Metric-based methods are primarily focused on learning feature embeddings that enable similarity comparisons between support and query images. The Prototypical Network [8] used a Euclidean distance measure to compare the feature embeddings of the query images with centroids of the support images in different classes. The Relation Network [9] constructed an additional network to compute the similarity score between images directly, instead of using the Euclidean distance measure on the images' feature embeddings similar to the Prototypical Network. DN4 [28] used a cosine similarity measure on multiple local descriptors, obtained by expanding the feature embeddings of the last layer to higher dimensions, to find the most similar images via nearest neighbor search.

2.1.2. Optimization-based Meta-learning

Optimization-based methods are focused on parameter optimization and how to rapidly learn knowledge from limited training images that can be adapted to novel images. The model agnostic meta-learning framework (MAML) [10] learned a general model that can be efficiently fine-tuned to perform well on other tasks using conventional gradient descent-based optimization. While MAML used second-order partial derivatives to train the general model before task-specific fine-tuning, Reptile [30] was a first-order approximation of MAML that simplified the training procedure and boosted computational performance. Ravi and Larochelle [11] introduced a related yet different approach to optimization-based meta-learning. They proposed the use of an LSTM to model the sequence corresponding to the sequential optimization of the model parameters across different tasks.

2.1.3. Graph-based Meta-learning

Graph-based meta-learning uses graph structures to model the relationship between query and support images based on relative similarity measures, where each labeled and unlabeled image represents a node in the graph. There are very few treatments of graph-based methods for FSL in the literature; however, the topic has recently gained more attention in the FSL research community.

In 2017, Garcia and Bruna [20] proposed the use of a graph neural network (GNN) for aggregating node information in an iterative fashion via a message-passing model, where the support and query images are densely connected in the graph. The edge-labeling graph neural network (EGNN) modified this approach, using edge- rather than node-label information, combined with inter-cluster dissimilarity and intra-cluster similarity measures [22]. Like GNN, the Transductive Propagation Network (TPN) considered the graph nodes for representing the feature embeddings of the images [21]. However, instead of performing inductive inference (that is, predicting test images one by one), TPN used transductive inference to predict the labels of the entire test set at once, which alleviated the low-data problem in FSL and achieved state-of-the-art performance [21].

2.2. Transfer Learning

In contrast to meta-learning, transfer learning is based on a more conventional supervised learning approach. Here, a model is pre-trained on a large dataset with an abundant number of examples per class. After pre-training on these base classes, the model is then transferred (i.e., fine-tuned) to the novel classes in a few-shot task.

The weight imprinting [12] method constructed classifiers for novel tasks by imprinting the centroids of the novel images' feature embeddings on classifier weights. TransMatch [25] extended this concept to semi-supervised settings. The dynamic few-shot object recognition system proposed by Gidaris and Komodakis introduced an attention module during training to learn the classifier weights [13]. The dense classification network was another method based on imprinting [29]. In addition, this method expanded the feature embeddings obtained, from the last layer, to a set of vectors when computing the cross-entropy loss during training on the base classes in the training. All cross-entropy loss terms were aggregated to compute the overall loss during backpropagation.

The Looking-Back method we propose in this paper (Figure 1) uses the same graph construction approach as TPN [21]. However, Looking-Back incorporates the feature embeddings from hidden layers in the graph construction procedure as well. We shall note that the simultaneous training with graphs built on lower-level information could also be seen as a particular case of multi-task learning or incremental learning, which was mentioned in [31] but is rarely adopted in FSL.

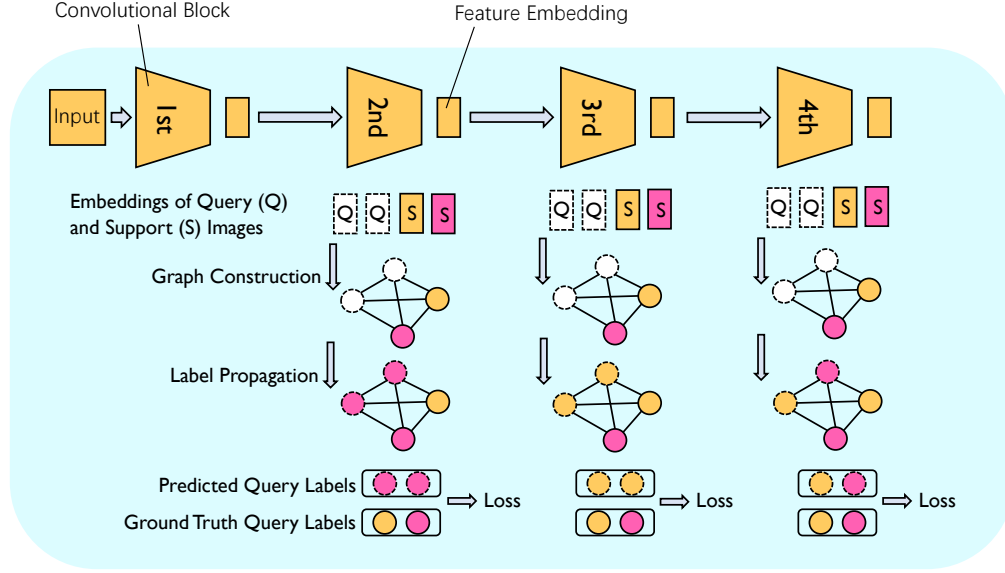


Figure 1. A conceptual overview of the proposed Looking-Back method.

3. Proposed Method

In this section, we introduce our proposed Looking-Back approach utilizing lower-level information to enhance the predictive performance of FSL models.

3.1. Problem Definition

The goal of FSL is to train predictive models that learn from and perform well on classification tasks, given only a few labeled examples per class. For instance, N -way K -shot classification can be understood as a classification task with K unique classes, where N labeled examples per class are provided for supervised learning.

In an N -way K -shot setting, the dataset for a given task is divided into a support set $\mathbf{S} = \{(\mathcal{X}_s, \mathcal{Y}_s)\}$ and a query set $\mathbf{Q} = \{(\mathcal{X}_q, \mathcal{Y}_q)\}$. \mathbf{S} consists of $N \times K$ examples $\mathcal{X} = (\mathbf{x}_1, \mathbf{x}_2, \dots, \mathbf{x}_{N \times K})$ and the corresponding class labels $\mathcal{Y} = (y_1, y_2, \dots, y_{N \times K})$. The goal is to utilize \mathbf{S} to predict the class labels $(y'_1, y'_2, \dots, y'_{Q \times K})$ for the $Q \times K$ examples in \mathbf{Q} , $(\mathbf{x}'_1, \mathbf{x}'_2, \dots, \mathbf{x}'_{Q \times K})$.

Given a large training dataset D_{base} , with base classes \mathbf{C}_{base} , FSL meta-learning approaches sample many different N -way K -shot classification tasks $\mathcal{T} = \{T_1, T_2, \dots, T_m\}$ randomly from D_{base} , to train the meta-learner for m episodes. After training, the meta-learner is given a novel N -way K -shot classification task T_{novel} , such that the K classes do not overlap with the base classes in D_{base} encountered during training. The dataset corresponding to T_{novel} is split into support and query sets, and the meta-learner uses the $N \times K$ labeled examples in the support set to classify the $Q \times K$ examples in the query set.

A successful FSL meta-learner learns from the training tasks T_1, T_2, \dots, T_m how to efficiently utilize the few labeled examples in the support set of a novel task T_{novel} so that the resulting model is able to predict the class labels in the unlabeled query set with good generalization performance.

Considering the general problem definition of FSL and meta-learning given above, the examples in the query set can be used in a transductive manner as suggested by [21]. I.e., instead of classifying the query examples one at a time, the whole query set can be propagated into the network all at once, which improves the predictive performance compared to classifying each query example independently [21].

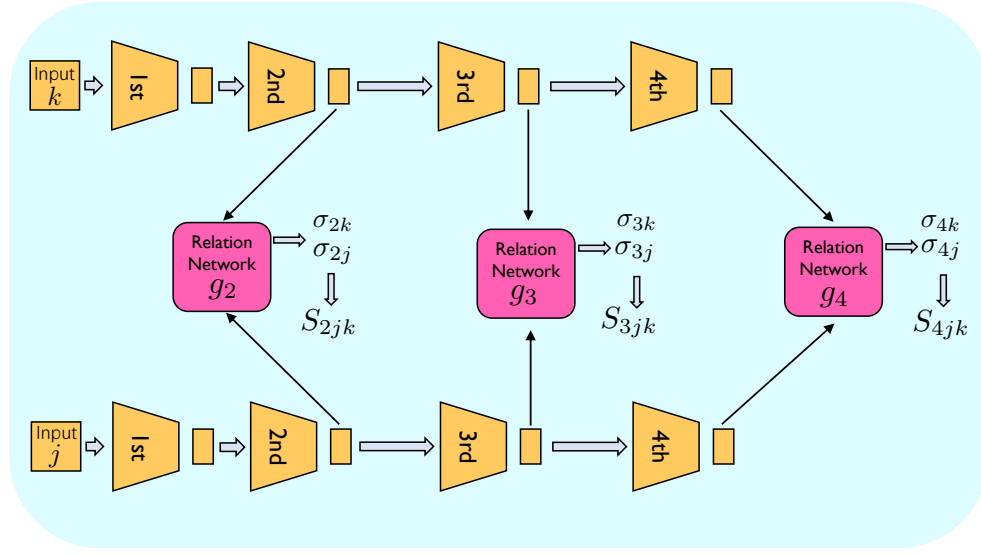


Figure 2. Computing the similarity between a pair of images, inputs j and k , based on the feature embeddings produced by the 2nd, 3rd, and 4th convolutional block (layer). The similarity values computing by the relation networks are then used to construct multiple graphs for transductive inference.

3.2. Feature Extractor Module

The two predominant types of neural network backbone architectures used in FSL research are ResNet-12 [32–35] and Conv-64F [7–9,20,21,28]. In this work, we adopt Conv-64F since it is easier to experiment with. However, we shall note that our proposed method is architecture-agnostic and can be implemented for other types of feedforward neural networks.

Conv-64F contains four convolutional blocks where every block is constructed by one convolutional layer with 64 filters of size 3×3 , followed by a batch normalization layer, ReLU activation, and a 2×2 max-pooling layer. Both the convolutional layers and the max-pooling layers have a stride of 1.

Besides extracting feature embeddings from the last layer of the last convolutional block, the proposed Looking-Back also extracts the embeddings from the last layer of the second and third convolutional block. These three feature embeddings are then used in the graph-based label propagation, as illustrated in Figure 1. The dimensions of the feature embeddings extracted by the three convolutional blocks are $64 \times 21 \times 21$, $64 \times 10 \times 10$, and $64 \times 5 \times 5$, respectively. Here, the number of channels, 64, is determined by the Conv-64F architecture, whereas the channel heights and widths are a consequence of the input image dimensions given the Conv-64F architecture.

3.3. Graph Construction Module

In the original work of TPN [21], the authors proposed a pair-wise similarity function that used an example-wise length-scale parameter. Adopting this mechanism, for the output of i -th convolutional block, we compute the similarity of two images (j, k) via

$$S_{ijk} = \exp \left(-\frac{1}{2} \left\| \frac{f_i(\mathbf{x}_{ij})}{\sigma_{ij}} - \frac{f_i(\mathbf{x}_{ik})}{\sigma_{ik}} \right\|_2^2 \right), \quad (1)$$

which measures the distance between the two feature embeddings. Here σ_{ij} is computed by a relation network module. As illustrated in Figure 2, we use a separate relation network for the second, third,

and fourth convolutional block, since the dimensions and information contents of the respective feature embeddings differ.

The overall architecture of the relation network module, which compute σ_{ij} and σ_{ik} , is similar to the architecture used in TPN [21]. For instance, each relation network module consists of two convolutional blocks, followed by two fully-connected layers. Each convolutional block is composed of a 3×3 convolutional layer with a stride of 1, a batch normalization layer, ReLU activation, and a 2×2 max-pooling layer with a stride of 1.

In the Looking-Back model, we compute multiple symmetric normalized graph Laplacians [36] via

$$L_i = D_i^{-1/2} S_i D_i^{-1/2}, \quad (2)$$

where D is the diagonal matrix whose d -th diagonal element is the sum of the d -th row of the i -th Laplacian $L_i \in \mathbb{R}^{(N \times K + Q) \times (N \times K + Q)}$. Similar to TPN, we keep the m -max values when constructing multiple m -nearest neighbor graphs during episodic training to improve computational efficiency.

3.4. Classification Loss

After constructing multiple nearest neighbor graphs as explained in Section 3.3, we use label propagation [37], similar to TPN [21], to compute the prediction (i.e., class-membership) scores for the query images.

Let $P^{(0)}$ be an initial score matrix. For a given image $\langle \mathbf{x}_j, y_j \rangle$ in the support set,

$$P_{jl}^{(0)} = \begin{cases} 0 & \text{if } y_j \neq l, \\ 1 & \text{if } y_j = l. \end{cases} \quad (3)$$

The label propagation process is an iterative process

$$P^{(t+1)} = \alpha L_i P^{(t)} + (1 - \alpha) P^{(0)}, \quad (4)$$

where $P^{(t)}$ is the predicted label at time step t . The predicted scores P_i^* for an input image's feature embedding from the i -th convolutional block are computed via

$$P_i^* = (I - \alpha L_i)^{-1} P^{(0)}, \quad (5)$$

where I is the identity matrix, L_i is the normalized graph Laplacian of that feature embedding from the i -th convolutional block, and α is a hyperparameter controlling propagation rate.

After computing the prediction scores, we obtain class-membership probability scores for the feature embeddings from the i -th convolutional block by applying a softmax function as follows:

$$p(\hat{y}_{ij} = k | \mathbf{x}_{ij}) = \frac{\exp(P_{i,jk}^*)}{\sum_{k=1}^N \exp(P_{i,jk}^*)}, \quad (6)$$

where \hat{y}_{ij} is the predicted class label for feature embedding of the j -th input image from the i -th convolutional block, and $P_{i,jk}^*$ is the predicted score at the k -th position.

The total loss term is the combination of cross-entropy loss for different layers' features:

$$\text{Loss} = - \sum_i \sum_{j=1}^{N \times K + Q} \sum_{k=1}^N w_i \mathbb{I}(y_{ij} = k) \log(p(\hat{y}_{ij} = k | \mathbf{x}_{ij})), \quad (7)$$

where w_i is a relative weight for the cross-entropy loss term of the feature embeddings from the i -th convolutional block and is a hyperparameter during the episodic training.

The feature embeddings from the second ($i = 2$) and third ($i = 3$) convolutional block containing lower-level information are only used during training to improve the feature extractor module (Section 3.2). In both the validation and test stage, the class labels $\hat{y} = \arg \max_k p(\hat{y}_i = k | \mathbf{x}_i)$ are obtained from the prediction on feature embeddings of the last convolutional block only, that is, the fourth convolutional block, $i = 4$.

4. Experiments

In this section, we evaluate the proposed Looking-Back method on two popular FSL benchmark datasets, i.e., *miniImageNet* [11] and *tieredImageNet* [23], and compare with other state-of-the-art FSL methods.

4.1. Datasets

miniImageNet. The *miniImageNet* dataset is widely used for comparing different few-shot learning methods [11]. It is a small subset of ImageNet [38] that consists of 100 classes with 600 examples per class. For our experiments, we split the dataset into 64 classes for training, 16 classes for validation, and 20 classes for testing following [11].

tieredImageNet. Similar to *miniImageNet*, the *tieredImageNet* dataset is a small, simplified version of ImageNet proposed by [23]. Different from *miniImageNet*, *tieredImageNet* has a hierarchical or *tiered* structure consisting of 34 larger classes, where each larger class contains 10 to 30 smaller classes (i.e., related subcategories). *tieredImageNet* contains 608 smaller classes and 779,165 images in total. We split the dataset as described in [23], resulting in a training set consisting of 20 larger classes, a validation set consisting of 6 larger classes, and the test set consisting of 8 larger classes. The advantage of splitting the dataset based on the larger classes, as opposed to splitting into the subclasses, is that this approach creates a clearer distinction between training, test, and validation sets.

4.2. Implementation Details

As mentioned before, we adopted the Conv-64F architecture (Section 3.2) as the backbone for our model. During training, we used the three layers' feature embeddings as shown in Figure 1 and Figure 2. For label propagation, we chose the same hyperparameters as described in [21], setting α (the propagation coefficient, Eq. 4 and 5) to 0.99 and m (the per-row max values of the graph Laplacians) to 20. Moreover, we gave equal weighting to the individual loss terms when computing the total loss Eq. 7, that is, setting w_2 , w_3 , and w_4 to 1.

During the episodic training, each episode was a 5-way K -shot task with 15-query images in each task, mimicking the testing scenario. We used the Adam optimizer [39] to train the model and set the initial learning rate to 0.001. For *miniImageNet*, the learning rate was decayed by a multiplicative factor of 0.8 every 5,000 episodes. The same multiplicative factor was used for decaying the learning rate when training on *tieredImageNet*, but it was decayed more frequently, every 2,000 epochs, due to the larger size and complexity of *tieredImageNet*.

To evaluate the model on the test set, we randomly sampled 600 5-way K -shot tasks from an independent test set with $K = 1$ and $K = 5$, respectively. In both scenarios, $K = 1$ and $K = 5$, there were 15 query samples in each class (that is, 75 query examples in total), which were used to compute the prediction accuracy for a given task or episode. To compute the overall prediction accuracy of a given model, we randomly sampled the test set 600 times and calculated the accuracy by averaging the prediction accuracy across these 600 episodes.

Table 1. Accuracy (in %) on *miniImageNet* with 95% confidence interval. Best results are shown in bold.

Method	Extract. Net.	1-shot	5-shot
Matching Net [7]	Conv-64	43.56 \pm 0.84	55.31 \pm 0.73
Prototypical Net [40]	Conv-64	49.42 \pm 0.78	68.20 \pm 0.66
Relation Net [9]	Conv-64	50.44 \pm 0.82	65.32 \pm 0.70
Reptile [30]	Conv-64	49.97 \pm 0.32	65.99 \pm 0.58
GNN [20]	Conv-64	49.02 \pm 0.98	63.50 \pm 0.84
MAML [10]	Conv-64	48.70 \pm 1.84	63.11 \pm 0.92
TPN [21]	Conv-64	53.75 \pm 0.86	69.43 \pm 0.67
Looking-Back	Conv-64	55.91 \pm 0.86	70.99 \pm 0.68

Table 2. Accuracy (in %) on *tieredImageNet* with 95% confidence interval. Best results are shown in bold.

Method	Extract. Net.	1-shot	5-shot
Prototypical Net [40]	Conv-64	53.31 \pm 0.89	72.69 \pm 0.74
Relation Net [9]	Conv-64	54.48 \pm 0.93	71.31 \pm 0.78
Reptile [30]	Conv-64	52.36 \pm 0.23	71.03 \pm 0.22
MAML [10]	Conv-64	51.67 \pm 1.81	70.30 \pm 1.75
TPN [21]	Conv-64	57.53 \pm 0.96	72.85 \pm 0.74
Looking-Back	Conv-64	58.97 \pm 0.97	73.59 \pm 0.74

4.3. Results and Discussion

Overall performance. In this section, we compare our proposed Looking-Back method to other state-of-the-art FSL methods. All neural network implementations are based on a Conv-64F backbone architecture for feature extraction as described in Section 3.2. Following the established conventions, we consider both 5-way 1-shot and 5-way 5-shot settings for the performance comparisons, using the two common FSL benchmark datasets *miniImageNet* and *tieredImageNet* as described in Section 4.1. The accuracy is computed as the average of 600 test episodes (as described in Section 4.2) with a 95% confidence interval. As the results for *miniImageNet* (Table 1) and *tieredImageNet* (Table 2) indicate, our proposed Looking-Back method achieves state-of-the-art results on both datasets, in both the 5-way 1-shot and 5-way 5-shot scenarios.

Comparing Looking-Back and TPN training in a "Higher Shot" setting. The performance comparisons between Looking-Back and TPN [21] (Table 1 and 2), provide supportive evidence that utilizing lower-level information, which is contained in previous layers' feature embeddings and utilized by Looking-Back, improves the predictive performance by a substantial amount. In this section, we investigate whether the lower-level information can also enhance the performance in a "Higher Shot" setting.

In FSL, it is common to use support sets of similar size during meta-training and testing. However, some researchers found that using larger support sets during meta-training (i.e., increasing the number of "shots") can improve the predictive performance of FSL systems based on evaluation on the same (i.e.,

Table 3. Accuracy (in %) after training with higher shots. Here, the system evaluated on a 1-shot test set was trained in a 5-shot setting, and the system evaluated on a 5-shot test set was trained in a 10-shot setting. Best results are shown in bold.

Dataset	Method	1-shot	5-shot
<i>miniImageNet</i>	TPN	55.51 \pm 0.86	69.86 \pm 0.65
	Looking-Back	56.49 \pm 0.83	70.47 \pm 0.66
<i>tieredImageNet</i>	TPN	59.91 \pm 0.94	73.30 \pm 0.75
	Looking-Back	61.19 \pm 0.92	73.78 \pm 0.74

Table 4. Performance gain (in % points) of Looking-Back vs TPN on the test sets when using lower-level information in same-shot (Same) and higher-shot (Higher) training.

Training approach	Dataset	1-shot	5-shot
Same	<i>miniImageNet</i>	2.16	1.56
	<i>tieredImageNet</i>	1.44	0.74
Higher	<i>miniImageNet</i>	0.98	0.61
	<i>tieredImageNet</i>	1.28	0.48

Table 5. Performance gain (in % points) of Looking-Back when trained with higher shots compared to training with same shots.

Dataset	1-shot	5-shot
<i>miniImageNet</i>	0.58	-0.52
<i>tieredImageNet</i>	2.22	0.19

smaller shot) test sets [8,28]. Similar observations have been made in the original TPN paper [21], where the authors described that increasing the number of examples in the support sets during meta-training (referred to as "Higher Shot") can improve the predictive accuracy during testing. However, using a larger number of shots during meta-training than testing does not always improve the predictive performance, and it is still an open area of research [41].

Although "Higher Shot" training is not the focus of this paper, we conducted experiments with higher shots and report the results in Table 3, adopting the procedure described in the original TPN paper [21] to enable fair comparisons. The results in Table 3 indicate that Looking-Back utilizing lower-level information outperforms TPN in a "Higher Shot" setting as well.

Table 4 summarizes the performance gain of Looking-Back over TPN for the regular meta-training scenario (same number of shots in the training and test tasks, Table 1 and 2) and meta-training with higher shots (Table 3). From Table 4, we can observe that on both datasets, the improvement of *same* versus *higher* shot meta-training in 1-shot settings is more significant than in 5-shot settings. We argue that when more support images are available (higher shot), the role of utilizing lower-level information becomes less important. The main rationale behind using previous layers' feature embeddings is to use additional lower-level information when information from the final layer's feature embedding is scarce. Intuitively, the role of using lower-level information degrades if a meta-learner can utilize a larger number of examples in the support set.

Influence of higher shot training on Looking-Back. As indicated by the results in Table 4 and hypothesized in the previous section, our Looking-Back method could be more useful when the data is more scarce. This is likely because the more information is available during training (i.e., the support sets consist of additional examples in higher-shot settings), the more negligible the information from earlier layers becomes as supportive information.

In a 1-shot setting, we were still able to observe that the lower-level information used by Looking-Back models benefits the model performance when training in the higher shots setting, as summarized in Table 5. However, in the presence of a larger number of images, using lower-level information during training results in more limited improvements (5-shot test setting on *tieredImageNet*) or may have a small detrimental impact (5-shot test settings on *miniImageNet*) as shown in Table 5. This finding provides further evidence that the lower-level information has a more beneficial effect when the data is more scarce.

Why only using the last layer's information during inference. Both DN4 [28] and the dense classification network [29] use the entire expanded feature embeddings of the last layer during training as well as inference. One of the main reasons we only use the feature embeddings of the last layer during inference is that the lower-level information from previous layers is used to augment the graph

Table 6. Different layers' prediction accuracy (in %) on 5-way tasks after label propagation with same-shot training.

Dataset	Setting	2nd layer	3rd layer	4th layer
<i>miniImageNet</i>	1-shot	42.24 \pm 0.76	50.87 \pm 0.81	55.91 \pm 0.86
	5-shot	58.10 \pm 0.72	67.07 \pm 0.69	70.99 \pm 0.68
<i>tieredImageNet</i>	1-shot	46.25 \pm 0.87	54.70 \pm 0.93	58.97 \pm 0.97
	5-shot	61.12 \pm 0.75	69.94 \pm 0.74	73.59 \pm 0.74

construction during training but does not have equal relevance for the prediction task during inference. In contrast to Looking-Back, in both DN4 and the dense classification network, the additional information of the expanded feature embeddings are on the same footing.

To test our hypothesis that the feature embeddings of the last layer bear the most relevance for the prediction task, we compared the prediction accuracy of Looking-Back when using different layers for the class label prediction. As indicated by the results in Table 6, the prediction accuracy of the 4th (last) layer is higher than the prediction accuracy of the 3rd layer, and the accuracy of the 3rd layer is higher than the accuracy of the 2nd layer, supporting the hypothesis that the last layer contains the most useful information.

5. Conclusion

In this paper, we propose a new approach to FSL, capturing additional information inside the feature extracting network to improve prediction performance. In particular, the proposed Looking-Back method employs a graphical structure to utilize the lower-level information from previous layers' feature embeddings, which differs from existing methods that only focus on expansions of the last layer's feature embeddings. Experiments on two popular FSL datasets provide evidence for the benefits of using lower-level information in FSL.

Author Contributions: Conceptualization, Z.Y., S.R.; investigation and validation, S.R., Z.Y.; data curation, Z.Y.; writing—original draft preparation, Z.Y., S.R.; writing—review and editing, Z.Y., S.R.; visualization, Z.Y., S.R.; supervision, S.R.; project administration, S.R.; funding acquisition, S.R. All authors have read and agreed to the published version of the manuscript.

Funding: Support for this review article was provided by the Office of the Vice Chancellor for Research and Graduate Education at the University of Wisconsin-Madison with funding from the Wisconsin Alumni Research Foundation.

Conflicts of Interest: The authors declare no conflict of interest.

References

1. Liu, L.; Ouyang, W.; Wang, X.; Fieguth, P.; Chen, J.; Liu, X.; Pietikäinen, M. Deep learning for generic object detection: A survey. *International Journal of Computer Vision* **2020**, *128*, 261–318.
2. Wani, M.A.; Bhat, F.A.; Afzal, S.; Khan, A.I. Supervised deep learning in face recognition. In *Advances in Deep Learning*; Springer, 2020; pp. 95–110.
3. Wang, W.; Liang, D.; Chen, Q.; Iwamoto, Y.; Han, X.H.; Zhang, Q.; Hu, H.; Lin, L.; Chen, Y.W. Medical image classification using deep learning. In *Deep Learning in Healthcare*; Springer, 2020; pp. 33–51.
4. Raschka, S.; Patterson, J.; Nolet, C. Machine learning in Python: Main developments and technology trends in data science, machine learning, and artificial intelligence. *Information* **2020**, *11*, 193.
5. LeCun, Y.; Bengio, Y.; Hinton, G. Deep learning. *Nature* **2015**, *521*, 436–444.
6. Wang, Y.; Yao, Q.; Kwok, J.T.; Ni, L.M. Generalizing from a few examples: A survey on few-shot learning. *ACM Computing Surveys* **2019**.
7. Vinyals, O.; Blundell, C.; Lillicrap, T.; Wierstra, D.; others. Matching networks for one shot learning. *Advances in Neural Information Processing Systems*, 2016, pp. 3630–3638.

8. Snell, J.; Swersky, K.; Zemel, R. Prototypical networks for few-shot learning. *Advances in Neural Information Processing Systems*, 2017, pp. 4077–4087.
9. Sung, F.; Yang, Y.; Zhang, L.; Xiang, T.; Torr, P.H.S.; Hospedales, T.M. Learning to compare: relation network for few-shot learning. *2018 IEEE/CVF Conference on Computer Vision and Pattern Recognition* **2018**, pp. 1199–1208.
10. Finn, C.; Abbeel, P.; Levine, S. Model-agnostic meta-learning for fast adaptation of deep networks. *International Conference on Machine Learning*, 2017, pp. 1126–1135.
11. Ravi, S.; Larochelle, H. Optimization as a model for few-shot learning. *International Conference on Learning Representations*, 2017.
12. Qi, H.; Brown, M.; Lowe, D.G. Low-shot learning with imprinted weights. *2018 IEEE/CVF Conference on Computer Vision and Pattern Recognition* **2018**, pp. 5822–5830.
13. Gidaris, S.; Komodakis, N. Dynamic few-shot visual learning without forgetting. *2018 IEEE/CVF Conference on Computer Vision and Pattern Recognition* **2018**, pp. 4367–4375.
14. Qiao, S.; Liu, C.; Shen, W.; Yuille, A.L. Few-shot image recognition by predicting parameters from activations. *2018 IEEE/CVF Conference on Computer Vision and Pattern Recognition* **2018**, pp. 7229–7238.
15. Scarselli, F.; Gori, M.; Tsoi, A.C.; Hagenbuchner, M.; Monfardini, G. The graph neural network model. *IEEE Transactions on Neural Networks* **2009**, *20*, 61–80.
16. Kipf, T.; Welling, M. Semi-supervised classification with graph convolutional Networks. *ArXiv* **2017**, *abs/1609.02907*.
17. Velickovic, P.; Cucurull, G.; Casanova, A.; Romero, A.; Liò, P.; Bengio, Y. Graph attention networks. *ArXiv* **2018**, *abs/1710.10903*.
18. Gilmer, J.; Schoenholz, S.S.; Riley, P.F.; Vinyals, O.; Dahl, G.E. Neural message passing for quantum chemistry. *Proceedings of the 34th International Conference on Machine Learning-Volume 70*, 2017, pp. 1263–1272.
19. Duvenaud, D.K.; Maclaurin, D.; Iparraguirre, J.; Bombarell, R.; Hirzel, T.; Aspuru-Guzik, A.; Adams, R.P. Convolutional networks on graphs for learning molecular fingerprints. *Advances in Neural Information Processing Systems*, 2015, pp. 2224–2232.
20. Garcia, V.; Estrach, J.B. Few-shot learning with graph neural networks. *6th International Conference on Learning Representations*, 2018.
21. Liu, Y.; Lee, J.; Park, M.; Kim, S.; Yang, E.; Hwang, S.J.; Yang, Y. Learning to propagate labels: transductive propagation network for few-shot learning. *International Conference on Learning Representations*, 2019.
22. Kim, J.; Kim, T.; Kim, S.; Yoo, C.D. Edge-labeling graph neural network for few-shot Learning. *2019 IEEE/CVF Conference on Computer Vision and Pattern Recognition* **2019**, pp. 11–20.
23. Ren, M.; Triantafillou, E.; Ravi, S.; Snell, J.; Swersky, K.; Tenenbaum, J.B.; Larochelle, H.; Zemel, R.S. Meta-Learning for semi-supervised few-shot Classification. *International Conference on Learning Representations*, 2018.
24. Li, X.; Sun, Q.; Liu, Y.; Zhou, Q.; Zheng, S.; Chua, T.S.; Schiele, B. Learning to self-train for semi-supervised few-shot classification. *Advances in Neural Information Processing Systems*, 2019, pp. 10276–10286.
25. Yu, Z.; Chen, L.; Cheng, Z.; Luo, J. TransMatch: A transfer-learning scheme for semi-supervised few-shot learning. *ArXiv* **2019**, *abs/1912.09033*.
26. Xing, C.; Rostamzadeh, N.; Oreshkin, B.; Pinheiro, P.O. Adaptive cross-modal few-shot learning. *Advances in Neural Information Processing Systems*, 2019, pp. 4848–4858.
27. Schonfeld, E.; Ebrahimi, S.; Sinha, S.; Darrell, T.; Akata, Z. Generalized zero-and few-shot learning via aligned variational autoencoders. *2019 IEEE/CVF Conference on Computer Vision and Pattern Recognition*, 2019, pp. 8247–8255.
28. Li, W.; Wang, L.; Xu, J.; Huo, J.; Gao, Y.; Luo, J. Revisiting local descriptor based image-to-class measure for few-shot learning. *2019 IEEE/CVF Conference on Computer Vision and Pattern Recognition* **2019**, pp. 7253–7260.
29. Lifchitz, Y.; Avrithis, Y.; Picard, S.; Bursuc, A. Dense classification and implanting for few-shot learning. *2019 IEEE/CVF Conference on Computer Vision and Pattern Recognition* **2019**, pp. 9250–9259.
30. Nichol, A.; Achiam, J.; Schulman, J. On first-order meta-learning algorithms. *ArXiv* **2018**, *abs/1803.02999*.

31. Mallya, A.; Lazechnik, S. PackNet: Adding multiple tasks to a single network by iterative pruning. *2018 IEEE/CVF Conference on Computer Vision and Pattern Recognition* **2018**, pp. 7765–7773.
32. Mishra, N.; Rohaninejad, M.; Chen, X.; Abbeel, P. A simple neural attentive meta-learner. *International Conference on Learning Representations*, 2018.
33. Oreshkin, B.; López, P.R.; Lacoste, A. TADAM: Task dependent adaptive metric for improved few-shot learning. *Advances in Neural Information Processing Systems*, 2018, pp. 721–731.
34. Lee, K.; Maji, S.; Ravichandran, A.; Soatto, S. Meta-learning with differentiable convex optimization. *2019 IEEE/CVF Conference on Computer Vision and Pattern Recognition*, 2019, pp. 10657–10665.
35. Sun, Q.; Liu, Y.; Chua, T.S.; Schiele, B. Meta-transfer learning for few-shot learning. *2019 IEEE/CVF Conference on Computer Vision and Pattern Recognition*, 2019, pp. 403–412.
36. Chung, F.R.; Graham, F.C. *Spectral graph theory*; American Mathematical Soc., 1997.
37. Zhou, D.; Bousquet, O.; Lal, T.N.; Weston, J.; Schölkopf, B. Learning with local and global consistency. *Advances in Neural Information Processing Systems*, 2004, pp. 321–328.
38. Deng, J.; Dong, W.; Socher, R.; Li, L.J.; Li, K.; Li, F.F. ImageNet: A large-scale hierarchical image database. *2009 IEEE/CVF Conference on Computer Vision and Pattern Recognition* **2009**, pp. 248–255.
39. Kingma, D.P.; Ba, J. Adam: A method for stochastic optimization. *ArXiv* **2014**, *abs/1412.6980*.
40. Fort, S. Gaussian prototypical networks for few-shot learning on omniglot. *ArXiv* **2018**, *abs/1708.02735*.
41. Cao, T.; Law, M.T.; Fidler, S. A theoretical analysis of the number of sShots in few-shot learning. *ArXiv* **2020**, *abs/1909.11722*.